JOURNAL OF COLLOID AND INTERFACE SCIENCE **179,** 439–448 (1996)
ARTICLE NO. 0235

Yielding and Flow of Monodisperse Emulsions

T. G. MASON,* J. BIBETTE,* AND D. A. WEITZ†,[1]

*Centre de Recherche Paul Pascal, Avenue A. Schweitzer, F-33600 Pessac, France; and †Department of Physics and Astronomy, University of Pennsylvania, Philadelphia, Pennsylvania 19104

Received June 26, 1995; accepted October 25, 1995

We have measured the yield transition of monodisperse emulsions as the volume fraction, ϕ, and droplet radius, a, are varied. We study the crossover from the perturbative shear regime, which reflects the linear viscoelastic properties, to the steady shear regime, which reflects nonlinear, plastic flow. For small oscillatory strains of peak amplitude γ, the peak stress, τ, is linearly proportional to γ. As the strain is increased, the stress becomes nonlinear in γ at the yield strain, γ_y. The ϕ dependence of γ_y is independent of a and exhibits a minimum near the critical volume fraction, $\phi_c \approx 0.635$, associated with the random close packing of monodisperse spheres. We show that the yield stress, τ_y, increases dramatically as the volume fraction increases above ϕ_c; τ_y also scales with the Laplace pressure, σ/a, where σ is the interfacial tension. For comparison, we also determine the steady shear stress over a wide range of strain rates, $\dot{\gamma}$. Below $\phi \approx 0.70$, the flow is homogeneous throughout the sample, while for higher ϕ, the emulsion fractures resulting in highly inhomogeneous flow along the fracture plane. Above $\phi \approx 0.58$, the steady shear stress exhibits a low strain rate plateau which corresponds with the yield stress measured with the oscillatory technique. Moreover, τ_y exhibits a robust power law dependence on $\dot{\gamma}$ with exponents decreasing with ϕ, varying from $\frac{2}{3}$ to $\frac{1}{2}$. Below $\phi \approx 0.58$, associated with the colloidal glass transition, the plateau stress disappears entirely, suggesting that the equilibrium glassy dynamics are important in identifying the onset of the yield behavior.

Key Words: **emulsions; rheology of emulsions; yield stress; yield strain; flow of emulsions.**

INTRODUCTION

Emulsions are dispersions of droplets of one fluid, such as oil, mixed into an immiscible continuous phase of another fluid, such as water. The addition of surfactant is necessary to provide a short-range repulsion between the oil–water interfaces which inhibits droplet coalescence and can stabilize the emulsion against demixing for many years. By mixing oil into a much smaller volume of aqueous surfactant solution, it is possible to form a concentrated emulsion comprised of highly deformed droplets. Such emulsions exhibit a plastic-like response to shear deformations; for small deformations, they resist the shear elastically, with the stress, τ, being linearly proportional to the strain, γ; however, for large enough deformations, they flow, offering comparatively much less additional resistance. For example, mayonnaise maintains its shape under the relatively small stresses of gravity, but it can be easily spread with a knife with little more effort. By contrast, at dilute concentrations as for example with milk, the droplets are undeformed, and emulsions exhibit simple viscous flow which closely resembles that of the dominant continuous phase. Since nearly all practical applications of emulsions require their transport, it is important to establish how their flow behavior is influenced by the properties of the constituent droplets, such as their packing, their degree of deformation, their volume fraction, ϕ, and their radius, a.

The flow properties of compressed, elastic emulsions can be broadly divided into two categories, yielding and steady shearing flow. The change from a linear to a nonlinear stress–strain relationship can be crudely characterized by a yield stress, τ_y, and a yield strain, γ_y, which mark the significant departure of the microscopic droplet structure from its initial, unsheared configuration. For $\tau > \tau_y$, the emulsion flows irreversibly, creating a residual deformation after the stress has been removed which cannot be attributed to the equilibrium dissipation of fluctuations. During steady shear flow, the strain rate dependence of the additional viscous stress, τ_v, above τ_y reflects the interplay of dissipative mechanisms like fluid flow and droplet rearrangements with storage mechanisms like deformation. Thus the flow properties of compressed emulsions depend sensitively on the packing and deformation of the droplets, and on their intrinsic elasticity. The elasticity of the droplets, and the degree of deformation, are controlled by their internal pressure, or the Laplace pressure, σ/a, where σ is the surface tension of the interfaces. Thus, this depends sensitively on the size of the droplets. Similarly, the packing of the droplets depends sensitively on the distribution of droplet sizes.

The flow properties of emulsions at lower volume fraction are also dependent on both the size of the droplets and the

[1] To whom correspondence should be addressed. Fax: (215) 898-2010. E-mail: weitz@dept.physics.upenn.edu.

0021-9797/96 $18.00

distribution of their sizes. At lower volume fractions, the droplets are uncompressed, and hence spherical in shape, in the absence of shear; they can be deformed by the shear itself if it is sufficiently large, although this generally requires excessively large values of the shear. Instead, the presence of their interfaces modifies the flow patterns within the fluid, thus increasing the dissipation, and hence the viscosity. However, exactly how this occurs depends sensitively on the nature of the hydrodynamic flow at their interfaces, as well as their volume fraction. Moreover, the nature of the hydrodynamic interactions induced by the droplets is very sensitive to the droplet size, as well as the distribution of sizes.

Since emulsions are not at thermodynamic equilibrium, their production requires the addition of energy to create the large interfacial area. This is typically provided by means of mixing, and the resultant emulsion possesses droplets with a wide range of sizes. Thus, the extreme sensitivity of all the flow properties of emulsions on their sizes and packing conditions, both in the compressed, high volume fraction limit and in the undeformed, low volume fraction limit, has made the study of their behavior very difficult. Moreover, it has precluded any detailed comparison with simple theoretical models, which generally assume a single droplet size. In this paper, we use emulsions with monodisperse droplets, obtained by a crystallization fractionation process (1), to study the flow properties of emulsions; this eliminates the complications due to the variation in the Laplace pressure of polydisperse droplets and simplifies the structure of the packing of the droplets. We measure the yield conditions of compressed emulsions as their droplet volume fraction, ϕ, and their droplet radius, a, are varied. We find that the yield stress, scaled by the Laplace pressure, and the yield strain, both exhibit a universal ϕ dependence, decreasing from $\phi \approx 1$ toward a critical volume fraction, ϕ_c, which corresponds to the random close packing of monodisperse, undeformed spheres. Even below ϕ_c, where the droplets are essentially undeformed, the yield stress and strain persist, and the behavior is similar to colloidal hard sphere suspensions in which entropic contributions to the rheology are important (2). In addition, we measure the ϕ dependence of the viscosity at very low volume fractions, when the droplets are not deformed and find that the surfactant coating of the droplets has sufficient elasticity to prevent the flow of the surfactant molecules on the surface. As a result, the emulsion droplets behave hydrodynamically as solid spheres, and the flow of the fluid is not transferred to the liquid within the droplets.

The flow properties of polydisperse emulsions have been extensively investigated in a comprehensive set of experiments using well-controlled samples (3, 4); however, the polydispersity of the droplets complicated microscopic interpretation of the data. The flow properties of emulsions have also been investigated theoretically (5) and through simulation (6–8); however, this work was focused on idealized emulsions that were both perfectly monodisperse and perfectly ordered. These investigations are useful in establishing the limiting behavior, but could not be compared with the experimental data in detail. Nevertheless, the periodicity of a perfectly crystalline emulsion facilitates the analysis because the resistance of a single droplet in a unit cell bounded by its neighbors and subjected to shear deformation completely describes the rheological response of the entire crystal. This simplification permits precise definitions of the yield stress and yield strain because the crystal fails catastrophically everywhere simultaneously. In the limit of very high volume fraction, the emulsion is composed of a network of thin films, and its stability under shear is determined entirely by the mechanical stability of the intersection of these films at the Plateau borders; three water films which meet at an edge must be separated by 120° angles, and four water films which meet at a corner must meet at tetrahedral angles (9, 10).

Any fully periodic single droplet model implies an abrupt drop of the stress, and global rearrangements in which complete rows slip by one another in unison, when the yield strain is exceeded. Thus, even a two-dimensional hexagonal array of deformable cylinders (5) captures the essential behavior of more complicated three-dimensional models. A static calculation of the dependence of the stress on the strain at a fixed ϕ shows a linear dependence at small strains, $\tau = G'\gamma$, where G' is the elastic modulus. For larger γ, the stress continues to increase with γ, but is no longer linear, instead increasing more slowly; this nonlinearity becomes more pronounced as ϕ decreases toward ϕ_c. Finally, at high enough γ, the stress drops abruptly, indicating global rearrangement; this defines the yield strain, γ_y. This yield strain rises discontinuously from zero to $\gamma_y \approx 0.2$ at ϕ_c, because perfectly packed spherical droplets must deform significantly before yielding due to their close interdigitation. Since both the elastic modulus and the yield strain rise abruptly at ϕ_c, the yield stress must also rise abruptly at ϕ_c.

The relationship between the behavior predicted by the models for emulsions with perfect crystalline order of the droplets and that observed for real emulsions with their disordered structure of the droplets can be put in context by considering the behavior of more traditional solids. In all materials except perfect crystals, the behavior of dislocations, or localized regions of structural disorder, is the basis for understanding yield properties and plastic flow (11). While the predicted yield strain for a perfect crystal composed of elements interacting through harmonic central forces is of order $\gamma_y \approx 0.1$, similar to the theory for purely repulsively interacting ordered arrays of emulsion droplets, most atomic or molecular crystals have much lower measured yield strains, typically below 10^{-4} (11). The weakness of real crystals is due to the inhomogeneous microscopic motion of dislocations which are absent in the idealized crystal. The density and orientation of dislocations control

the degree of weakness; thermal energy and the past shear history create, destroy, and align them. Predictions from dislocation theory for disordered polycrystalline materials are in reasonable agreement with the measured yield strains of $\gamma_y \approx 10^{-2}$ in many work-hardened metals, alloys, and polycrystalline materials. This highlights the critical role played by disorder, which can sharply reduce the yield strain of any crystalline lattice; this should apply equally well to emulsions and is essential in understanding our results.

MATERIALS AND METHODS

In our experiments, we use silicone oil-in-water emulsions, stabilized with sodium dodecyl sulfate (SDS). These emulsions are purified using a fractionation procedure (1); this results in highly monodisperse droplets after about five fractionation steps. The remaining polydispersity is less than 10% of the radius, and the droplets are sufficiently monodisperse that some crystalline order is observed in samples that are maintained at volume fractions of about 0.5 for several weeks. We study emulsions with different radii, $a = 0.25$, 0.37, 0.53, and 0.74 μm. The continuous phase water is maintained at an SDS concentration of $C = 10$ mM, which is high enough to maintain the stability of the emulsions against coalescence, yet low enough to eliminate any attractive interaction due to depletion of the micelles. The oil viscosity for each emulsion is $\eta_o = 12$ cP, except for the emulsion with a = 0.53 μm, which has $\eta_o = 230$ cP. In all cases, the surface tension is measured to be $\sigma = 9.8$ dyn/cm. All measurements are made at room temperature.

An initial reservoir of highly concentrated emulsion is obtained by centrifugation, and samples at the desired volume fractions are obtained by diluting portions of the reservoir sample using a solution of 10 mM SDS in water. The volume fraction remains constant during the course of the measurements since creaming of the emulsion in the rheometer is negligible due to the small droplet sizes and the relatively short time over which the measurements are performed. Although they can form ordered lattices at some volume fractions, all the experiments reported here are performed using samples that are disordered on a macroscopic length scale, as determined by light scattering (12). The droplet volume fraction of each sample is determined by weighing the sample before and after evaporation of the water. To determine the effective volume fraction of the packing, we must account for both the volume of the oil in the droplets as well as the volume of the thin film of water, of thickness, h, which always exists between the droplets, due to the stabilizing electrostatic repulsion of the SDS. Thus, we define an effective volume fraction, which we approximate as $\phi_{\text{eff}} \approx \phi(1 + 3h/2a)$, which determines the packing of the droplets (13). For $\phi < \phi_c$, $h \approx 175$ Å, as found in force–distance measurements using ferrofluid emulsions coated with the same surfactant (14). The film thickness decreases to $h \approx 50$ Å near $\phi \approx 1$; this is consistent with the Debye length of the double-layer repulsion between the highly deformed interfaces and a disjoining pressure of σ/a. To determine ϕ_{eff}, we linearly interpolate between these two values as ϕ is varied (13). As a result of this additional film of water, the value of the effective packing volume fraction differs from the true droplet volume fraction by a few percent; however, the exact amount depends on the droplet size.

Our measurements are performed using a mechanical controlled-strain rheometer equipped with a vapor trap to prevent water evaporation (15). At high volume fractions, we employ a cone and plate geometry, but for $\phi \leqslant 0.60$, we use a double-wall Couette geometry which has a larger surface area, thereby increasing the rheometer's stress sensitivity. We completely eliminate any slip at the walls of the rheometer by using sand blasting to roughen their surfaces on length scales ranging from 5 to 500 μm, which are comparable to, or larger than, the droplet diameter. We also ensured that no slip occurred preferentially at the walls at higher strains or strain rates and ascertained that the measured bulk properties are independent of gap thickness in the cone and plate geometry and that the measurements on a given sample are reproducible when the sample is reloaded into the rheometer. In addition, the emulsion was checked after the measurements and no evidence of coalescence was found, either at the walls or in the bulk. The latter could be reliably determined by observing the emulsion with a microscope, because of the monodisperse droplet size (16). These precautions ensured the absence of wall slip. This simplifies the interpretation of our data and contrasts with a more complicated technique which purposefully introduces wall slip and later corrects for it (17). The loading of the emulsion into the sample cell necessarily induces a large preshear perpendicular to the direction of the azimuthally applied strain. This preshear is radial for the cone and plate, and axial for the double-wall Couette.

We employ two different rheological techniques; a perturbative oscillatory measurement is followed by a steady shear measurement. The oscillatory measurement is made by sweeping the strain up to $\gamma \approx 3$ at a fixed frequency; this precisely determines the yield stress and yield strain, but it also causes the emulsion to yield along the flow direction. This is followed by a steady shear measurement at a fixed strain rate which is useful for determining the yield stress and the viscous stress. The oscillatory measurement is best adapted for determining the yield strain because the departure from the linear regime of rheology is controlled, while the steady shear measurement is best adapted for measuring the viscous stress because the strain rate is controlled.

RESULTS AND DISCUSSION

For the oscillatory measurement, a sinusoidal strain, of peak amplitude, γ, is applied at a frequency, ω, and the

peak magnitude, $\tau(\omega)$, and temporal phase lag of the zero crossing, $\delta(\omega)$, of the resultant periodic stress response is measured. We illustrate the strain dependence of the stress and phase lag for an emulsion with $a = 0.53$ μm at $\phi = 0.70$ at $\omega = 1$ rad/s in Figs. 1a and 1b. At the lowest strains, the stress is linear in the strain, $\tau \sim \gamma$, the phase lag is independent of the strain, and the stress waveform is sinusoidal. In this regime, the linear complex shear modulus can be defined as, $G^*(\omega) = [\tau(\omega)/\gamma]e^{i\delta(\omega)}$; the real part is the storage modulus, $G'(\omega)$, which reflects the elasticity of the emulsion, while the imaginary part is the loss modulus, $G''(\omega)$, which reflects the dissipation (18). We plot these quantities as functions of γ in Fig. 1c. At the smallest γ, both G', shown by the solid symbols, and G'', shown by the open symbols, are independent of γ, reflecting the linear behavior; here they are related only to the equilibrium microscopic structure, forces, and inherent dissipation of fluctuations. However, for large enough γ the emulsion begins to yield, and the temporal dependence of the stress becomes nonsinusoidal, exhibiting flattened peaks (19); nevertheless, the peak stress has a robust sublinear power-law dependence on γ, while the phase lag reflects more dissipation by increasing dramatically from nearly zero toward $\pi/2$. When the stress–strain relationship is sublinear, the linear storage and loss moduli are no longer strictly appropriate descriptions of the emulsion rheology because they begin to depend strongly on γ. Nevertheless, as shown in Fig. 1c, we can still plot the apparent moduli at higher values of γ.

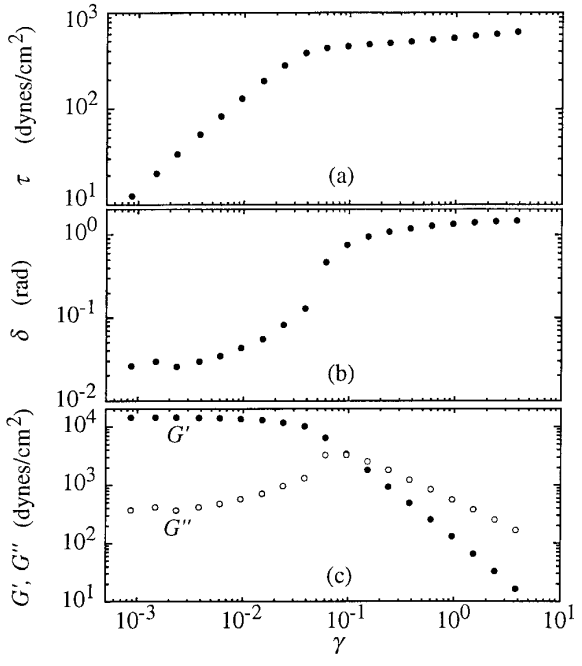

FIG. 1. Oscillatory shear measurement at $\omega = 1$ rad/s of (a) the peak stress, τ, (b) the phase lag, δ, and (c) the storage modulus, G', (solid circles) and loss modulus, G'', (open circles) as a function of peak strain, γ, for a concentrated emulsion with radius $a = 0.53$ μm and volume fraction $\phi = 0.70$. At the lowest γ, the stress response is sinusoidal, while at the highest γ, it is nonsinusoidal.

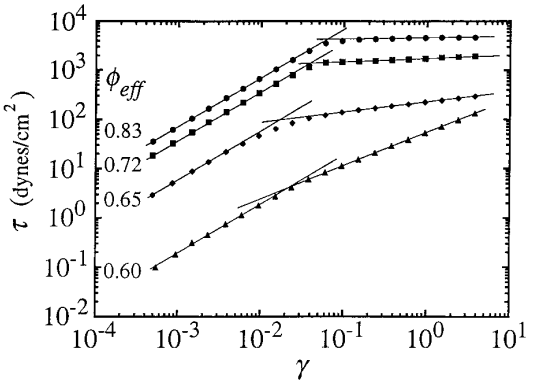

FIG. 2. The peak stress τ (solid symbols) plotted as a function of the peak strain γ at $\omega = 1$ rad/s for a monodisperse emulsion having radius $a = 0.53$ μm from $\phi_{\text{eff}} = 0.60$ to $\phi_{\text{eff}} = 0.83$. At each ϕ_{eff}, a line having slope one on the log–log plot is extrapolated through the data at low γ until it intersects, at the yield stress τ_y and yield strain γ_y, with a line of lower slope drawn through the data at high γ.

A similar, sublinear power law in the peak stress–strain relationship is observed at high γ for all volume fractions of the emulsion, as shown in Fig. 2; these data were obtained with the emulsion with $a = 0.53$ μm and were measured at $\omega = 1$ rad/s. This power law reflects the departure from dominantly elastic behavior and the increased dissipation due to irreversible deformation. Since the nonlinear flow is modified by the geometry and volume fraction, the value of the exponent is difficult to interpret. However, since the power law is robust, existing over several orders of magnitude in γ, we can conveniently define a yield stress, τ_y, and yield strain, γ_y, by the intersection of the extrapolations of the low strain linear power law and the high strain sublinear power law, as shown by the solid lines in Fig. 2. While this criterion is quite natural and well defined, alternative criteria using the strain dependence of δ, G', and G'' could be used instead. This criterion allows us to measure the variation of the yield parameters with volume fraction; as shown in Fig. 2, the yield strain varies weakly with ϕ_{eff}, but the yield stress increases many orders of magnitude for increasing ϕ_{eff}.

Considerable insight into the nature of the yielding behavior is gained from the study of the dependence on the droplet size, and hence the internal Laplace pressure. The dependence of the yield strain on ϕ_{eff} is plotted in Fig. 3 for all droplet sizes. The volume fraction dependence of the yield strain is independent of a and exhibits a pronounced minimum near ϕ_c. This behavior indicates that it is the geometry of the droplet packing, and their resultant deformations, that are responsible for the volume fraction dependence of the yield strain. The volume fraction dependence of γ_y is also insensitive to frequency and to the viscosity of the oil. At the minimum, $\gamma_y \approx 0.025$, indicating that the emulsion yields for minute relative droplet displacements that are much less

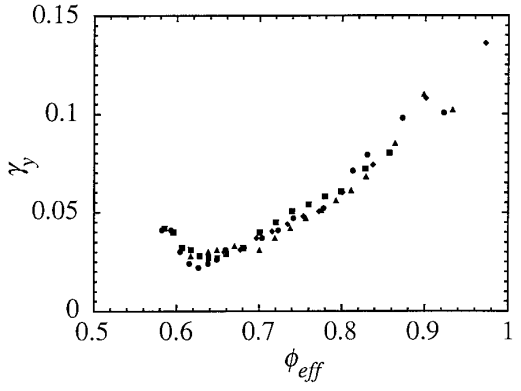

FIG. 3. The yield strain γ_y as a function of effective volume fraction for monodisperse emulsions having radii $a = 0.25$ μm (circles), 0.37 μm (triangles), 0.53 μm (squares), and 0.74 μm (diamonds).

than a diameter. This minimum occurs at $\phi_{\text{eff}} = 0.63$, which, given the experimental error in measuring ϕ_{eff}, is indistinguishable from the volume fraction of random close packing of undeformed spheres, ϕ_c (20, 21). Below ϕ_c, the yield strain increases to $\gamma_y \approx 0.045$ near $\phi_{\text{eff}} = 0.58$; however, the yield stress continues to decrease and measurements at lower ϕ_{eff} are limited by the stress resolution of our rheometer. Above ϕ_c, the yield strain increases to more than $\gamma_y \approx 0.1$ as ϕ_{eff} approaches 1; droplet coalescence prevents measurements at higher ϕ_{eff}.

The yield stress exhibits markedly different behavior. Like the yield strain, the data for all the droplets sizes can also be scaled together; however, in this case, we must first normalize the stress by the Laplace pressure of the droplets, σ/a, which sets the scale for all the stresses in the emulsion. This is shown in Fig. 4, where we plot the ϕ_{eff} dependence of τ_y for all the droplets sizes; the scaling behavior is apparent. This scaling behavior is a key experimental verification that the scale of the yield stress is indeed set by the Laplace pressure, provided that the effective packing volume fraction of the droplets is used to incorporate the electrostatic repulsion between them. The independence of the scaled yield stress on droplet size is consistent with its definition as the product of the yield strain and scaled plateau shear modulus (2, 13), which are both universal, independent of a. By contrast to the gradual increase of the yield strain with volume fraction above ϕ_c, the yield stress rises much more dramatically. These data also establish the measured yield stress of real highly compressed emulsions for comparison with theory; in the limit as $\phi_{\text{eff}} \to 1$, the yield stress approaches $0.1\ \sigma/a$, about one-sixth the measured limit for G'. Although τ_y rises sharply near ϕ_c, it is not as pronounced as the linear rise in the modulus (13) due to the increasing contribution of the yield strain toward larger ϕ_{eff}. Above ϕ_c, the scaled yield stress can be empirically fit by a quadratic form, $\tau_y/(\sigma/a) = C(\phi_{\text{eff}} - \phi_c)^2$, as shown by the solid line in Fig. 4 with $C = 0.51$ and $\phi_c = 0.62$. This is not surprising, since γ_y and G' each rise nearly linearly above ϕ_c; thus their product, the scaled yield stress, is well described by this quadratic form. This dependence is significantly weaker than predictions for perfectly ordered emulsions in which the yield stress jumps discontinuously to nearly σ/a immediately above ϕ_c (5). However, at high ϕ, the scaled yield stresses are about an order of magnitude greater than those measured for polydisperse emulsions (4).

Our measured yield strains are similar to observations of $\gamma_y \sim 10^{-2}$ for disordered molecular materials (11). Polydisperse emulsions at high ϕ have yield strains that are over an order of magnitude smaller (4). By comparison, computer simulations of three dimensional ordered droplets predict $\gamma_y \approx 0.6$ (8). This suggests that the droplet disorder, rather than polydispersity, is responsible for the lower yield strain of real emulsions, compared to theoretical predictions for perfectly ordered emulsions. Such idealized emulsions can yield only by a global topological rearrangement at a strain near unity; by contrast, the lower γ_y measured for these monodisperse, but disordered emulsions suggests that the disorder permits local rearrangements of droplets or groups of droplets. At $\phi \approx 1$, we can combine the prediction of $\gamma_y \approx 0.6$ from simulations on three-dimensional emulsions (8) with the measured value of $G' \approx 0.6\sigma/a$ (13), which compares well to the prediction of $G' = 0.55\ \sigma/a$ from a recent calculation of random films (22). We can then determine the predicted yield stress to be $0.3\ \sigma/a$ at $\phi \approx 1$. This is three times larger than we observe, suggesting that localized inhomogeneous flow of groups of droplets along weak planes introduced by the disorder weakens the structure of even highly compressed emulsions.

We hypothesize that the rise of the yield strain with droplet concentration above ϕ_c is due to a combination of disorder and increased packing constraints. The shear introduces localized microscopic motion of groups of packed droplets; these groups irreversibly slip relative to neighboring groups

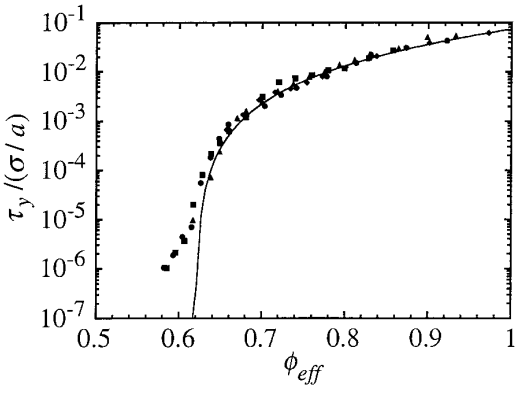

FIG. 4. The yield stress, τ_y, scaled by the Laplace pressure, σ/a, as a function of effective volume fraction for monodisperse emulsions having radii $a = 0.25$ μm (circles), 0.37 μm (triangles), 0.53 μm (squares), and 0.74 μm (diamonds). The data are essentially independent of droplet size. The solid line shows the scaled to a quadratic behavior, $(\phi_{\text{eff}} - \phi_c)^2$.

along weak planes or grain boundaries introduced by disorder. At low volume fractions near ϕ_c, there are many dislocations due to the randomness of the packing. At higher volume fractions, there are fewer weak planes and the packed groups become larger, because there is less water to distribute among the boundaries. Since the grain boundaries remain randomly oriented, the yield strain rises toward the theoretical estimate for a perfect crystal due to the larger domain size. However, if the grain boundaries had been oriented by a preshear along the direction of the strain, then one would expect the yield strain to drop because such orientation facilitates microscopic flow. This picture is similar in spirit to the picture of a rigidity loss which has been proposed to account for the ϕ_{eff} dependence of the static elastic modulus, $G'(\phi_{\text{eff}})$ (23); there, the existence of weaker regions, whose number increases as ϕ_{eff} approaches ϕ_c, accounts for the linear scaling of modulus, $(\phi_{\text{eff}} - \phi_c)$.

Below ϕ_c, the droplets no longer need to deform in order to pack; in fact there is additional free volume, which increases as $[a(\phi_c - \phi_{\text{eff}})]^3$ (24) as the volume fraction decreases below that of random close packing. Because of their Brownian motion, each droplet can explore the free volume accessible to it, and this contributes to the entropy, and hence to the total free energy of the system. Thus this provides an additional mechanism for energy storage; the applied shear strain can modify the shape of the free volume, thereby increasing the energy, and thus storing energy in the form of an elastic modulus. This is entirely entropic in nature, and provides a mechanism that can account for the elastic modulus of hard spheres below ϕ_c (2); a similar mechanism applies for the undeformed emulsion droplets below random close packing (13). Thus, the average intersurface separation also decreases with decreasing free volume; it should vary linearly as $a(\phi_c - \phi_{\text{eff}})$. Since this distance sets the maximum strain that can be applied before the behavior becomes nonlinear, we expect that the yield strain should also decrease to a minimum as $(\phi_c - \phi_{\text{eff}})$; similar behavior is observed for nondeformable hard spheres. While the emulsion data qualitatively agree with this, they do not vanish at ϕ_c because the droplets can deform. This permits a continuous crossover to the regime of dislocation motion which dominates above ϕ_c. This picture also implies that the scale for the yield stress below ϕ_c is set by the thermal energy density, k_BT/a^3, where k_B is Boltzmann's constant and T is the temperature. For $a \approx 0.5$ μm at room temperature, k_BT/a^3 is 5 dyn/cm^2, many orders of magnitude lower than the Laplace scale of 5×10^5 dyn/cm^2, but consistent with the measured yield stresses over the volume fraction range where we observe γ_y to rise. This also accounts for the disagreement of the empirical quadratic form with the data for the scaled τ_y below ϕ_c. Finally, we note that since this behavior is purely entropic in origin, it should make considerably less contribution for emulsions with significantly larger droplets, where the entropic energy density is much less.

While oscillatory measurements are useful for measuring emulsion yield properties, they cannot be used to determine the nonlinear flow. Instead, we characterize this flow by fixing a constant strain rate, $\dot{\gamma}$, and measuring the resultant stress when the total strain displacement is well in excess of the yield strain. The large deformations caused by the flow induce changes in the droplet structure; these affect the emulsion's resistance to flow until a self-consistent ''dynamic'' steady state is reached. This dynamic equilibrium may create inhomogeneous spatial variations in the strain rate within the emulsion, precluding a simple description using a single homogeneous strain rate. The homogeneity of the strain is determined experimentally by painting a stripe on the exposed surface of the emulsion before shearing and watching its evolution during shear (17). For $\phi_{\text{eff}} < 0.70$ and $a = 0.25$ μm, the painted stripe deforms continuously both below and above the yield strain. However, for higher ϕ_{eff}, an abrupt discontinuity in the stripe develops when the strain exceeds the yield strain, indicating inhomogeneous flow and the existence of a yield surface. Due to the significant roughness of the rheometer walls, the yield surface appears randomly within the gap. Its thickness is only a small fraction of the gap distance, and the strain rate is nearly zero everywhere in the emulsion except at the yield surface. Thus, the strain rate within the yield surface is much higher than the quoted strain rate which spatially averages over the inhomogeneous flow.

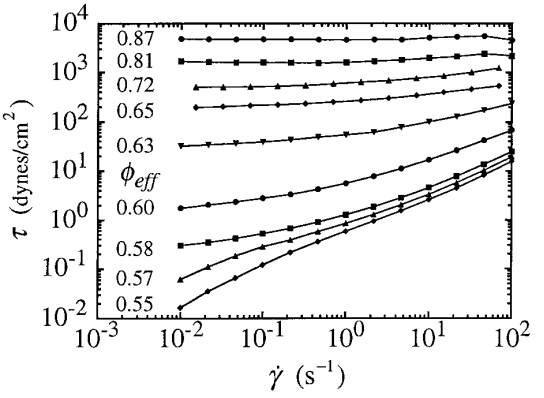

FIG. 5. The variation of the steady shear stress, τ, with strain rate, $\dot{\gamma}$, for $a = 0.25$ μm from $\phi_{\text{eff}} = 0.55$ to $\phi_{\text{eff}} = 0.88$. For $\phi_{\text{eff}} < 0.72$, the strain rate shown is a true homogeneous strain rate, but for $\phi_{\text{eff}} \geq 0.72$, the strain field is inhomogeneous, so the actual strain rates are not well defined. The solid lines guide the eye.

We measure the total stress resisting the steady flow as a function of strain rate for the emulsion with $a = 0.25$ μm by sweeping from $\dot{\gamma} = 10^{-2}$ s^{-1} to $\dot{\gamma} = 10^2$ s^{-1}. The results for a series of volume fractions between $0.55 \leq \phi_{\text{eff}} \leq 0.87$ are shown in Fig. 5. At any given value of strain rate, there is a large variation in the resistive stress, which increases by many orders of magnitude from the lowest to highest ϕ_{eff}. For $\phi_{\text{eff}} > 0.70$, where the flow becomes inhomogeneous, the stress is nearly independent of the quoted strain rate; we

emphasize, however, that the true strain rate in the thin yield surface can be larger than the quoted value by as much as a factor of 10. At the highest ϕ_{eff}, the stress does not vary smoothly with the strain rate due to the inhomogeneous flow. For $0.58 < \phi_{\text{eff}} < 0.70$, where the flow is homogeneous, the stress increases with the strain rate continuously from a plateau at $\dot{\gamma} = 10^{-2}\ \text{s}^{-1}$. We define a steady shear yield stress by the plateau stress at the lowest measured strain rate. Interestingly, there appears to be a well-defined transition at $\phi_{\text{eff}} \approx 0.58$, below which the plateau disappears completely. For lower volume fractions, the stress continues to drop as $\dot{\gamma}$ decreases; this corresponds to the appearance of inflection points and the complete disappearance of the plateau yield stress.

The dependence of the steady shear stress on $\dot{\gamma}$ well below $\phi_{\text{eff}} \approx 0.58$ reflects the time scales of stress relaxation of the equilibrium suspension. For $\phi_{\text{eff}} \leqslant 0.57$, the appearance of inflection points and disappearance of the plateau in the shear stress at low $\dot{\gamma}$ are evidence that the droplets partially relax to an unsheared configuration in less than 100 s. Since this occurs well below random close packing, the droplets are undeformed, and this relaxation is driven by Brownian motion. Moreover, since the droplets rearrange faster than the shear can perturb them, the plateau stress does not exist at $\dot{\gamma} = 10^{-2}\ \text{s}^{-1}$. This relaxation corresponds with changes in the frequency dependence of $G'(\omega)$ and $G''(\omega)$ determined by oscillatory measurements as ϕ_{eff} decreases below 0.55 (13). The frequency independent plateau in the storage modulus, observed for higher ϕ_{eff}, disappears for $\phi_{\text{eff}} \leqslant 0.55$, while the loss modulus rises at low frequencies. This comparison with the linear regime requires the yield stress to be related to the equilibrium shear modulus, $\tau_y = |G^*|\gamma_y$. Although for strongly compressed emulsions $|G^*|$ is essentially the frequency independent plateau value of G', for weakly compressed emulsions, $|G^*|$ varies with frequency, so the equilibrium dynamics of stress relaxations can affect τ_y.

The sudden disappearance of the plateau in the stress shear-rate measurements at $\phi_{\text{eff}} \approx 0.58$ suggests that the emulsion remains a solid, at least at these frequencies, down to this volume fraction. This is consistent with an ergodic to nonergodic colloidal glass transition occurring at $\phi_{\text{eff}} \approx 0.58$. This observation is supported by other experimental evidence of a glass transition. The frequency dependence of the linear moduli is well described (13) using a theory for the rheology of colloidal particles near the glass transition which has successfully described the behavior of hard spheres (2); this picture employs mode coupling theory (25) to describe the dynamics. Similarly, dynamic light scattering measurements of index matched emulsions also suggest the presence of a glass transition near $\phi_{\text{eff}} \approx 0.58$, and can also be well described using the predictions of mode coupling theory (12). Thus, for $\phi_{\text{eff}} \geqslant \phi_g$, a static yield, or plateau stress exists at arbitrarily low $\dot{\gamma}$. For ergodic suspensions below ϕ_g, it is possible, in principle, to wait long enough after the application of the strain for the stresses to relax, precluding the existence of a static yield stress. We emphasize, however, that the onset of a static yield strain occurs at the colloidal glass transition, $\phi_g \approx 0.59$, rather than the volume fraction of random close packing of undeformed spheres, $\phi_c \approx 0.63$.

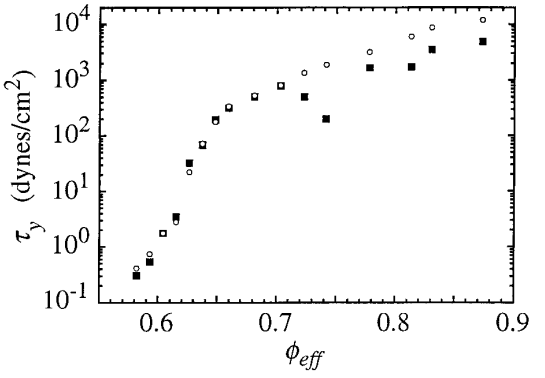

FIG. 6. A comparison of the yield stress, τ_y, determined by steady shear (solid squares) and oscillatory rheology measurements (open circles) as a function of ϕ_{eff} for an emulsion with radius $a = 0.25\ \mu$m. The steady shear τ_y is determined from the plateau at the strain rate of $\dot{\gamma} = 10^{-2}\ \text{s}^{-1}$ in Fig. 5, and the oscillatory τ_y is determined from the knee in the peak stress–strain relationship at $\omega = 1$ rad/s as in Fig. 2.

We compare the yield stresses measured as a function of ϕ_{eff} using the steady shear and the oscillatory techniques for the emulsion with $a = 0.25\ \mu$m in Fig. 6. There is excellent agreement between the two methods for $\phi_{\text{eff}} \leqslant 0.70$, indicating that either method is suitable for determining the yield stress there. At higher volume fractions, the steady-state measurement of the yield stress is typically about a factor of 3 lower than the dynamic oscillatory method, although there is some variation at different ϕ_{eff} due to the inhomogeneous flow. This suggests that the steady shear yield stress is consistently lower because the oscillatory test to $\gamma = 3$ precedes the steady shear measurement, aligning the dislocations along the direction of flow. Moreover, this observation, when combined with the visual observations of the stripe painted on the emulsion, provides considerable evidence that at a packing volume fraction of $\phi_{\text{eff}} \approx 0.70$, the nature of the nonlinear flow changes dramatically. However, the fundamental origin and significance of this volume fraction, which marks the broad transition from homogeneous to inhomogeneous flow and also from history-independent to history-dependent flow, is not clear.

Once an emulsion has yielded, it will flow at some finite strain rate, $\dot{\gamma}$. Attempts have been made to understand how much additional stress is required to produce a given strain rate once the yield strain has been exceeded. This relationship would be useful in many practical applications involving the transport of concentrated emulsions. However, since the strain rate is inhomogeneous at volume fractions approaching unity, the dependence of the additional viscous

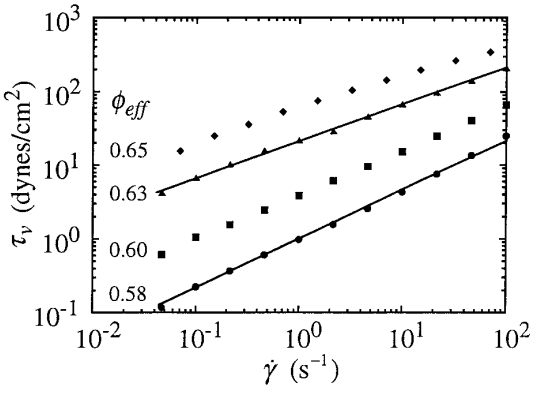

FIG. 7. The viscous stress, τ_v, as a function of strain rate, $\dot{\gamma}$, for an emulsion with radius $a = 0.25$ μm from $\phi_{\text{eff}} = 0.58$ to $\phi_{\text{eff}} = 0.65$. The viscous stress is obtained by subtracting the yield stress, measured at the lowest strain rate, from the total measured stress. The line drawn through the data for $\phi_{\text{eff}} = 0.58$ has slope $\frac{2}{3}$, while the line for $\phi_{\text{eff}} = 0.63$ has slope $\frac{1}{2}$.

stress cannot be determined. Nevertheless, it is possible to calculate the viscous stress, τ_v, for the four lowest volume fractions, where the yield stress exists and the flow is homogeneous. This is accomplished by subtracting the steady shear yield stress from the total measured stress. The viscous stress rises as a power law in the strain rate, with the exponent depending on ϕ_{eff}, as shown in Fig. 7. The slope decreases with ϕ_{eff} from about $\frac{2}{3}$ given by the solid line at $\phi_{\text{eff}} = 0.58$ to about $\frac{1}{2}$ given by the line at $\phi_{\text{eff}} = 0.63$. These slopes are insensitive to variations in the value of the yield stress used in the subtraction because the data span many decades. For $\phi_{\text{eff}} \geqslant 0.65$, the slopes of τ_v are less than $\frac{1}{2}$ at low $\dot{\gamma}$, and they deviate from a power law at high $\dot{\gamma}$.

Power law behavior of the viscous stress has been predicted for plastic creeping flow of a two-dimensional, ordered emulsion near $\phi \approx 1$ (26). The local flow of water around highly deformed droplets results in a bulk flow with a viscous stress that varies as $\dot{\gamma}^{2/3}$; this is confirmed by simulation (6, 7). However, this prediction neglects the inhomogeneous nature of the flow which is observed for real emulsions at such volume fractions, thereby precluding a direct comparison. Given the assumption of high compression, it is not surprising that this prediction disagrees with the observed exponent of $\frac{1}{2}$ at $\phi_{\text{eff}} = 0.63$, corresponding to loosely packed droplets. The $\dot{\gamma}^{1/2}$ behavior of τ_v has also been seen in polydisperse emulsions at higher volume fractions between $0.84 < \phi < 0.98$ (4). The increase in our observed power law exponent toward $\frac{2}{3}$ at lower ϕ_{eff} indicates a trend toward purely viscous behavior expected for dilute suspensions, which would have a slope of unity. This observation emphasizes that as ϕ_{eff} decreases well below ϕ_c, there must ultimately be a crossover to purely viscous behavior with no yield stress and τ_v proportional to $\dot{\gamma}$.

Finally, the availability of monodisperse droplets also allows us to critically test the predictions of the behavior of suspensions of liquid droplets under shear in the limit of low volume fractions. For such dilute suspensions, there is a prediction by Taylor (27) that the Newtonian viscosity of a suspension of fluid droplets, η, varies as

$$\eta = \eta_w \left[1 + \frac{5}{2} \phi \, \frac{(2/5\, \eta_w + \eta_o)}{(\eta_w + \eta_o)} \right];$$

here η_w and η_o are the viscosities of the continuous water and the droplet oil phases, respectively. When $\eta_o \gg \eta_w$, the reduces to the familiar Einstein expression for hard spheres, $\eta = \eta_w(1 + \frac{5}{2}\phi)$ (24). By contrast, when $\eta_w \gg \eta_o$, so that the internal droplet phase is much less viscous than the continuous phase, this reduces to $\eta = \eta_w(1 + \phi)$, which differs considerably from the Einstein prediction. Inherent in the Taylor expression is the assumption that stress is transmitted freely through the droplet interfaces, coupling the flows inside and outside. However, this assumption ignores the interfacial behavior of the surfactant, which may prevent such coupled flows.

This predicted behavior can be unambiguously tested since the droplets in these emulsions are monodisperse. Thus, we measure the ϕ dependence of the viscosities of monodisperse emulsions for $\phi < 0.25$ in the two limiting cases of $\eta_o \gg \eta_w$ and $\eta_o \ll \eta_w$. By restricting the measurements to low shear rates, we remain in the creeping flow limit where the droplets are not significantly deformed by the shear. There, the emulsion viscosity, measured as $\eta = \tau(\dot{\gamma})/\dot{\gamma}$, is independent of the strain rate between $10^1 < \dot{\gamma} < 10^2\ \text{s}^{-1}$. In addition, to determine if convection dominates diffusion, we consider the Peclet number (24), $\text{Pe} = \dot{\gamma}a^2/D_s(\phi)$, where $D_s(\phi)$ is the ϕ-dependent short time self diffusion coefficient; this the ratio of the relaxation rate due to convection to that due to diffusion. For dilute suspensions, the Stokes–Einstein relation, $D_s = k_BT/6\pi a\eta_w$, provides a good estimate of the diffusion coefficient. For $a = 0.55$ μm and $\eta_w = 0.997$ cP, $\text{Pe} \gg 1$ for all measured $\dot{\gamma}$, so η represents a high frequency viscosity. In Fig. 8, we plot with the circles the dimensionless relative viscosities, $\eta_r = \eta/\eta_w$, at different volume fractions for an emulsion with an oil having a viscosity of $\eta_o = 110$ cP, much larger than η_w. Our results agree well with a fit (28) to measurements and simulations for the high frequency viscosity of uniform hard spheres, given by the solid line. We also measure the opposite limit, $\eta_o \ll \eta_w$, for a monodisperse emulsion by adding glycerol to the water phase and using a lower viscosity oil; the relative viscosities for $\eta_w = 104$ cP, $\eta_o = 12$ cP, and $a = 0.20$ μm are shown by the squares in Fig. 8. These data are also similar to hard spheres and disagree with Taylor's asymptotic prediction for a much less viscous dispersed phase, shown by the dashed line.

This disagreement can be reconciled if tangential stress transmission through the droplet interfaces is prevented by

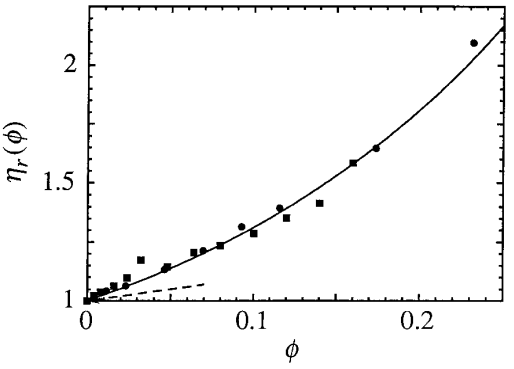

FIG. 8. The volume fraction dependence of the relative viscosity, η_r, for monodisperse emulsions with $a = 0.55$ μm, $\eta_o = 110$ cP, and $\eta_w = 0.997$ cP (circles) and $a = 0.20$ μm, $\eta_o = 12$ cP, and $\eta_w = 104$ cP (squares). The solid line is a fit (28) to measurements and simulations of hard sphere relative viscosity, and the dashed line is the asymptotic low ϕ prediction of Taylor (27) when $\eta_w \gg \eta_o$.

the immobilization of the surface through the Gibbs surface elasticity, E_N, of the surfactant. For SDS at $C = 10$ mM, $E_N \approx 10$ dyn/cm (29). Local gradients in the surface surfactant concentration set up by viscous flow create a restoring stress of magnitude E_N that counteracts the flow; this is known as the Marangoni effect. The tangential viscous stress acting on the droplet, $\eta_w a\dot{\gamma}$, is much less than E_N for $\dot{\gamma} < 10^6\ \mathrm{s}^{-1}$, so the surfactant on the droplet surfaces is immobilized. This prevents the coupling of the flow of the oil within the droplets to the flow of the water, and the emulsion behaves as a hard sphere suspension at the strain rates used in our experiments. Since the surface elasticity plays a significant role in the stability of the emulsion, we expect that stable emulsions made using other kinds of surfactants should also exhibit suspension viscosities that are well described by the theory for hard spheres at low volume fractions, rather than by the expression due to Taylor (27).

CONCLUSION

Using monodisperse droplets, we have demonstrated that the volume fraction dependencies of the yield strain and scaled yield stress are independent of droplet size. These key observations establish that the precise nature of the droplet packing and the Laplace pressure scale, σ/a, are the important microscopic properties which determine the yield behavior in emulsions. The association of the sharp rise in the yield stress above the volume fraction of random close packing is strong evidence that the disordered configuration of the droplet packing plays a key role in the yield properties of emulsions. This fact has been obscured in measurements using polydisperse emulsions due to the complex droplet packing.

The yield strain exhibits a pronounced minimum at the volume fraction of random close packing of undeformed spheres, $\phi_c \approx 0.63$. We account for this by hypothesizing the existence of two different regimes governing the yield properties of colloidal emulsions, depending on the degree of droplet packing and deformation. Above ϕ_c, the rise in the ϕ dependence of the yield strain suggests that the microscopic motion of randomly oriented dislocations between groups of highly deformed droplets becomes more strongly impeded as the emulsion becomes more highly compressed due to the increase in the volume fraction. The disorder accounts for the relative weakness of the observed yield properties compared to predictions for perfectly ordered crystalline emulsions. It also accounts for the history dependence of the yield stress in the most compressed emulsions; by aligning the dislocations along the direction of the shear, the yield stress is significantly reduced. In the other regime, below ϕ_c, the emulsion droplets are undeformed, so their yield properties and steady shear viscosities resemble those of hard sphere suspensions in which Brownian motion is important. The correspondence of the relaxation time scales of the steady shear $\tau(\dot{\gamma})$ and $|G^*|(\omega)$, and the disappearance of the plateau yield stress at volume fractions associated with the colloidal glass transition is further evidence for this similarity. Here the yield strain increases as ϕ decreases, reflecting the increasing separation between the particles. By contrast, the yield stress continues to decrease. We find that the static yield behavior disappears completely at $\phi_g \approx 0.58$, the colloidal glass transition. Finally, even at dilute concentrations, the emulsion viscosity is identical to that of hard sphere suspensions, suggesting that the surface elasticity of the surfactant is the primary reason why this correspondence can be made so generally. This qualitative picture of two regimes, while speculative, captures the essential features of the data, and it may ultimately provide a basis for a realistic theory of emulsion yielding and flow.

ACKNOWLEDGMENTS

This work was performed while the authors were with Exxon Research and Engineering Co. We have benefited greatly from conversations with Eric Herbolzheimer and Paul Chaikin. We thank NASA for partial support of this work.

REFERENCES

1. Bibette, J., *J. Colloid Interface Sci.* **147,** 474 (1991).
2. Mason, T. G., and Weitz, D. A., *Phys. Rev. Lett.* **75,** 2770 (1995).
3. Princen, H. M., and Kiss, A. D., *J. Colloid Interface Sci.* **112,** 427 (1986).
4. Princen, H. M., and Kiss, A. D., *J. Colloid Interface Sci.* **128,** 176 (1989).
5. Princen, H. M., *J. Colloid Interface Sci.* **91,** 160 (1983).
6. Reinelt, D. A., and Kraynik, A. M., *J. Colloid Interface Sci.* **132,** 491 (1989).
7. Reinelt, D. A., and Kraynik, A. M., *J. Fluid Mech.* **215,** 431 (1990).
8. Kraynik, A. M., and Reinelt, D. A., *J. Proc. XIth Int. Congr. Rheol.* 675 (1992).
9. Plateau, J. A. F., ''Statque Experimentale et Theorique des Liquides

Soumis aux Seules Forces Moleculaire.'' Gauthier–Villars, Paris, 1873.
10. Thomson, W. L. K., *Philos. Mag.* **25,** 503 (1887).
11. Kittel, C., ''Introduction to Solid State Physics,'' 6th ed. Wiley, New York, 1986.
12. Krall, A., Gang, H., and Weitz, D. A., submitted for publication.
13. Mason, T. G., Bibette, J., and Weitz, D. A., *Phys. Rev. Lett.* **75,** 2051 (1995).
14. Calderon, F. L., Stora, T., Monval, O. M., Poulin, P., and Bibette, J., *Phys. Rev. Lett.* **72,** 2959 (1994).
15. Whorlow, R. W., ''Rheological Techniques.'' Ellis Horwood, Chichester, 1980.
16. Bibette, J., Morse, D. C., Witten, T. A., and Weitz, D. A., *Phys. Rev. Lett.* **69,** 2439 (1992).
17. Princen, H. M., *J. Colloid Interface Sci.* **105,** 150 (1985).
18. Bird, R. B., Armstrong, R. C., and Hassager, O., ''Dynamics of Polymeric Liquids.'' Wiley, New York, 1977.
19. Yoshimura, A. S., and Prud'homme, R. K., *Rheol. Acta* **26,** 428 (1987).
20. Scott, G. D., *Nature* **188,** 908 (1960).
21. Bernal, J. D., and Mason, J., *Nature* **188,** 910 (1960).
22. Stamenovic, D., *J. Colloid Interface Sci.* **145,** 255 (1991).
23. Bolton, F., and Weaire, D., *Phys. Rev. Lett.* **65,** 3449 (1990).
24. Russel, W. B., Saville, D. A., and Schowalter, W. R., ''Colloidal Dispersions.'' Cambridge Univ. Press, Cambridge, 1989.
25. Götze, W., and Sjogren, L., *Rep. Prog. Phys.* **55,** 241 (1992).
26. Schwartz, L. W., and Princen, H. M., *J. Colloid Interface Sci.* **118,** 201 (1987).
27. Taylor, G. I., *Proc. R. Soc. London A* **138,** 41 (1932).
28. Ladd, A. J. C., *J. Phys. Chem.* **93,** 3484 (1990).
29. Bonfillon, A., and Langevin, D., *Langmuir* **9,** 2172 (1993).